Available online at www.sciencedirect.com
ScienceDirect
Trans. Nonferrous Met. Soc. China 28(2018) 1484−1494
Transactions of Nonferrous Metals Society of China
www.tnmsc.cn

Prediction on hot deformation behavior of spray-formed 7055 aluminum alloy via phenomenological models

Xiang-dong WANG[1], Qing-lin PAN[1], Shang-wu XIONG[2], Li-li LIU[1], Yuan-wei SUN[1], Wei-yi WANG[1]

1. School of Materials Science and Engineering, Central South University, Changsha 410083, China;
2. School of Light Alloys Research Institution, Central South University, Changsha 410083, China

Received 13 April 2017; accepted 9 December 2017

Abstract: Hot compression tests in the temperature range of 340−450 °C and strain rate range of 0.001−1 s^{-1} of spray-formed 7055 aluminum alloy were carried out to study its hot deformation behavior. Three phenomenological models including Johnson−Cook, modified Fields−Backofen and Arrhenius-type were introduced to predict the flow stresses during the compression process. And then, a comparative predictability of the phenomenological models was estimated in terms of the relative errors, correlation coefficient (R), and average absolute relative error (AARE). The results indicate that Johnson−Cook model and modified Fields−Backofen model cannot well predict the hot deformation behavior due to the large deviation in the process of line regression fitting. Arrhenius-type model obtains the best fit through combining the effect of strain rate and temperature.

Key words: spray-formed 7055 aluminum alloy; hot deformation behavior; phenomenological models; statistical analyses

1 Introduction

7xxx series of aluminum alloys are generally used in the aerospace field, vehicle manufacture and advanced weapon system due to a combination of good mechanical strength, high fracture and corrosion resistant [1−3]. Generally, these series of aluminum alloys will be subjected to various hot forming processes to attain better properties. The hot deformation is a complex dynamic process. Some parameters such as temperature, strain rate and strain can affect microstructure evolution by a combination of strain hardening and softening mechanisms [4]. In turn, microstructure evolution during hot deformation process has influence on some mechanical parameters and hence determines the final process. It is important to acquire knowledge on the flow behaviors of metals and alloys so as to optimize mechanical properties as well as avoid instabilities by understanding flow pattern and kinetics of metallurgical transformation such as dynamic recovery (DRV) and dynamic recrystallization (DRX).

Since there is not much experience in processing spray-formed 7055 aluminum alloy at elevated temperatures in industry and trial and the error in the workshop costs too much, it is of great importance to use numerical simulations to predict the forming process. For accurate simulation of the hot extrusion process, it is very necessary to understand the hot deformation behavior of material. Therefore, proper constitutive models that describe the relations among forming temperature, strain, strain rate and flow stress during deformation are required.

Based on tested data, there are several ways to model deformation behavior. Some phenomenological models and some physical-based models are generated to describe the flow stress as a function of the deformation path, temperature and strain rate. A phenomenological model often consists of convenient mathematical functions. There exist many phenomenological models including Johnson−Cook (JC) model, Fields−Backofen (FB) model, Arrhenius equation, and some other models [4]. For the past decades, Johnson−Cook model has been successfully used to show elevated temperature flow behavior of materials [5−7]. However，the original JC model was not able to predict the softening part of the flow curves owing to the uncoupled nature of the approach regarding strain rate and temperature [8]. Initially, Johnson−Cook model was established by JOHNSON and COOK [9] to present constitutive

Foundation item: Project (2013HH100055) supported by the Basic Research and Science and Technology Innovation Fund of Foshan City, China
Corresponding author: Qing-lin PAN; Tel/Fax: +86-731-88830933; E-mail: PQL1964@yeah.net
DOI: 10.1016/S1003-6326(18)64789-2

behavior when materials are subjected to large strains, high strain rates and high temperatures. To date, Johnson−Cook model is successfully used for a variety of materials with different ranges of forming temperature and strain rate. Fields−Backofen model, another phenomenological model, has been successfully introduced to describe stress−strain relationship. This model can well present the work hardening phenomenon by the strain hardening exponent and strain rate sensitivity exponent [10−12]. Since firstly proposed by FIELDS and BACHOFEN, the origin formula was revised to express softening behavior by considering the effect of strain rate by the strain rate sensitivity [13]. TAKUDA et al [14] modified the original model with strain rate sensitivity exponent and stress coefficient and verified that the formula gave a good fit to the AZ31 magnesium alloy. QUAN et al [15] also invited this model to describe the relations among flow stress, strain rate and temperature of 7075 aluminum alloy. However, the detailed prediction has not been reported. Arrhenius-type constitutive model, which considers the combined effects of strain rate and temperature on flow stress, can predict stress values under all kinds of high-temperature deformation conditions [16−18]. YAN et al [19] used this model to predict the high-temperature deformation behavior of an Al−Zn−Mg−Mn−Zr alloy precisely.

In this work, the hot deformation behavior of the spray-formed 7055 aluminum alloy was tested under different hot compression conditions. Three constitutive models of Johnson−Cook (JC), modified Fields−Backofen (FB), Arrhenius-type were established to determine the relationship amongst flow stress, strain, strain rate and temperature. The accuracy and effectiveness of these models were compared based on statistics indicators such as relative errors, correlation coefficient (R), and average absolute relative error (AARE).

2 Experimental

The compositions of the spray-formed 7055 aluminum alloy are listed in Table 1. The alloy was fabricated in Hao-ran Co. Ltd., Jiangsu, China. The cylindrical specimens were processed at dimensions of d10 mm × 15 mm. Both ends of the specimen were covered with graphite to minimize fraction between the device and specimen during deformation. The compression tests were carried out on a Gleeble−3500 thermal simulation device at 340, 370, 410 and 450 °C with strain rate ranging from 0.001 to 1.0 s^{-1}. Figure 1 shows the detailed procedure of these tests. The sample was heated at a rate of 2 °C/s and the specimen was held at the given temperatures for 3 min before compression. The collected data were then used to construct constitutive models to predict flow stress.

Table 1 Chemical compositions (mass fraction, %) of studied alloy (Fe and Si, associated with primary aluminum, are present as impurities)

Zn	Mg	Cu	Mn	Zr	Si	Fe	Al
7.91	1.98	2.42	0.004	0.12	0.082	0.096	Bal.

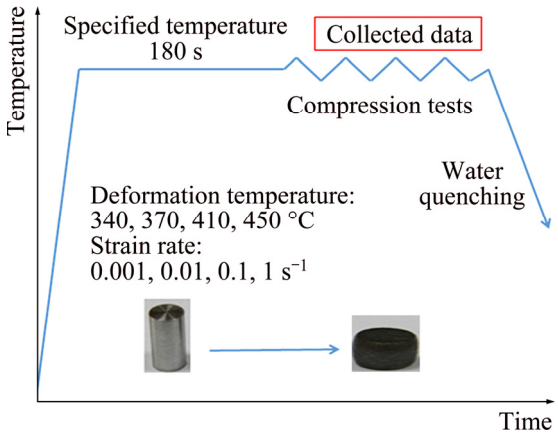

Fig. 1 Schematic diagram of hot compression tests

3 Results and discussion

3.1 Flow behavior

Figure 2 exhibits the true stress−true strain curves of spray-formed 7055 aluminum alloy deformed at temperatures of 340, 370, 410, 450 °C and strain rates of 0.001, 0.01, 0.1 and 1 s^{-1}. The flow stress increases immediately with increasing strain at the beginning of compression and then remains nearly constant or exhibits a slight decrease after reaching the peak stress. Work hardening due to dislocations multiply is the main reason of flow stress rising. The appearance of steady or decreased stage can be attributed to the paradoxical process of work hardening and dynamic softening such as dynamic recovery and dynamic recrystallization.

3.2 Johnson−Cook model

Johnson−Cook (JC) model was used in various materials due to its simple mathematical expression. The formula can be written as [9,20]

$$\sigma = (A + B\varepsilon^n)(1 + C\ln\dot{\varepsilon}^*)[1 - (T^*)^m] \quad (1)$$

where ε is the equivalent plastic strain; σ is the equivalent flow stress; A, B, n, C and m are material constants, in which A is the yield stress at reference temperature and strain, B is the coefficient of strain hardening, n is the strain hardening exponent, C is the coefficient of strain-rate hardening exponent and m is the coefficient of thermal softening exponent; $\dot{\varepsilon}^*$ is the dimensionless strain rate and can be represented as $\dot{\varepsilon}^* = \dot{\varepsilon}/\dot{\varepsilon}_0$, where $\dot{\varepsilon}$ is the strain rate and $\dot{\varepsilon}_0$ is the reference strain rate.

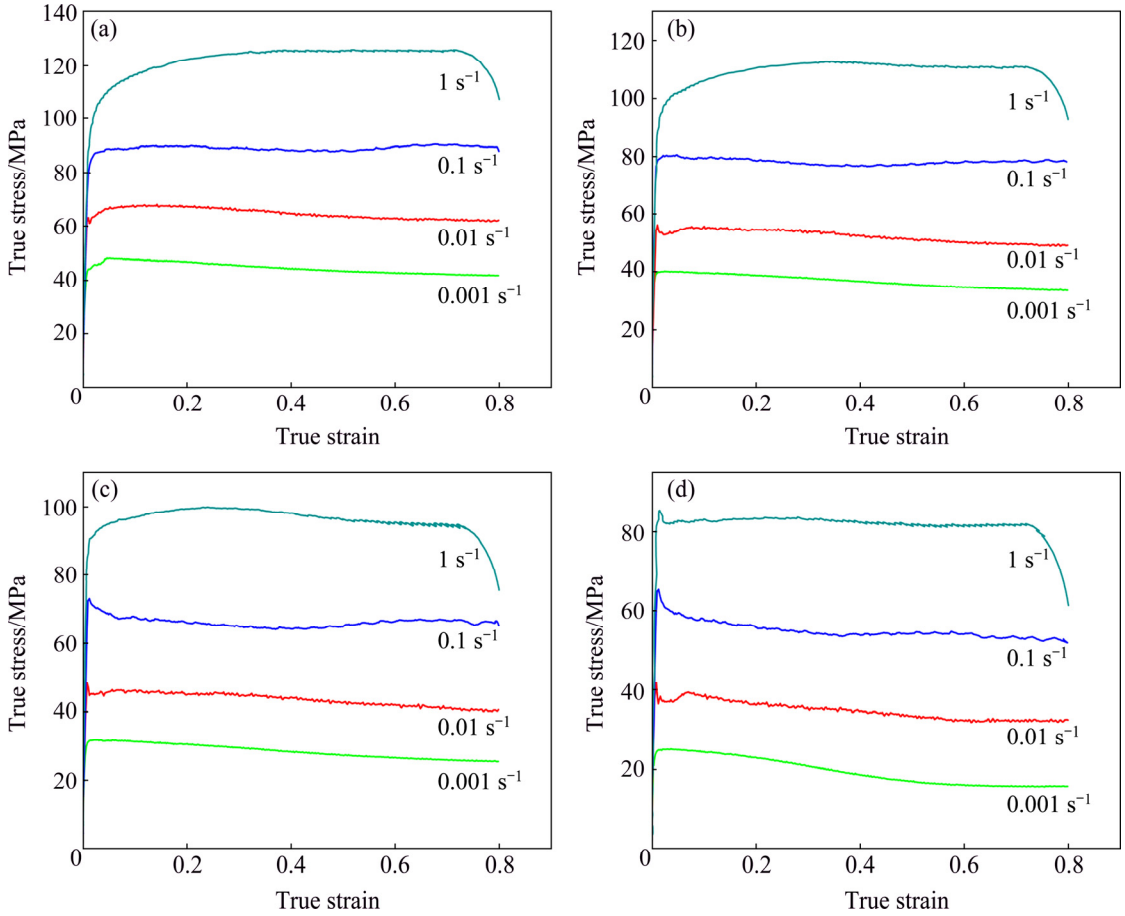

Fig. 2 True stress−true train curves of spray-formed 7075 aluminum alloy at different deformation temperatures: (a) 340 °C; (b) 370 °C; (c) 410 °C; (d) 450 °C

The homologous temperature, T^*, is expressed as

$$T^* = \frac{T - T_r}{T_m - T_r} \tag{2}$$

where T is the current absolute temperature, T_m is the melting temperature and T_r is the reference temperature. Usually, the minimum temperature is taken as the reference temperature ($T \geq T_r$). From Eq. (1), it can be drawn that the equivalent flow stress is divided into three items, where $(A+B\varepsilon^n)$, $(1+C\ln\dot{\varepsilon}^*)$ and $[1-(T^*)^m]$ are used for presenting the work hardening effect, strain rate effect and temperature effect, respectively.

In this experiment, the reference temperature was T_r=613 K and reference strain rate was $\dot{\varepsilon}_0$=0.01 s^{-1}. Under this condition, the yield stress was σ_0=68.24 MPa.

3.2.1 Determination of constant B and n

At the reference temperature and strain rate, Eq. (1) will be transformed into

$$\sigma = A + B\varepsilon^n \tag{3}$$

Taking natural logarithm on both sides of Eq. (3) gives

$$\ln(\sigma_0 - \sigma) = \ln(-B) + n\ln\varepsilon \tag{4}$$

Using the flow stress data at various strains for the same flow curves, $\ln(\sigma_0-\sigma)$ versus $\ln\varepsilon$ can be plotted, as shown in Fig. 3. B can be obtained from the intercept of this plot as −12.8971 while n is obtained from the slope to be 1.6093.

3.2.2 Determination of constant C

At reference temperature of 613 K, T^* can be calculated to be 0 according to Eq. (2). Then, Eq. (1) is expressed as

$$\sigma = (A + B\varepsilon^n)(1 + C\ln\dot{\varepsilon}^*) \tag{5}$$

Rearrange Eq. (5) to the form as follows:

$$\frac{\sigma}{A + B\varepsilon^n} = 1 + C\ln\dot{\varepsilon}^* \tag{6}$$

Figure 4 shows the relationship between $\sigma/(A+B\varepsilon^n)$ and $\ln\dot{\varepsilon}^*$ for different strains and strain rates at reference temperature. The mean value of constant C is obtained to be 0.1750 by linear regression.

3.2.3 Determination of constant m

When the strain rate is at reference value of 0.01 s^{-1}, Eq. (1) can be represented as

$$\sigma = (A + B\varepsilon^n)[1 - (T^*)^m] \tag{7}$$

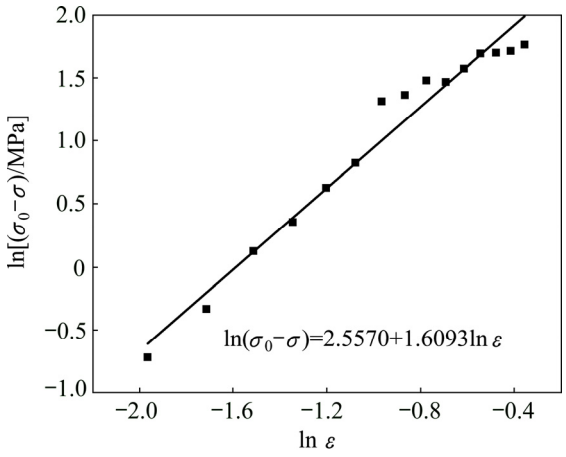

Fig. 3 Relationship between $\ln(\sigma_0-\sigma)$ and $\ln \varepsilon$

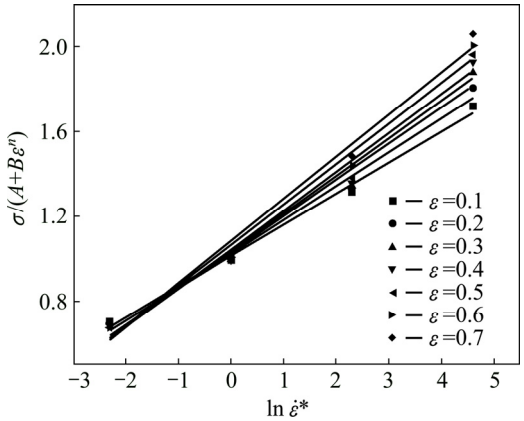

Fig. 4 Relationship between $\sigma/(A+B\varepsilon^n)$ and $\ln \dot{\varepsilon}^*$

Rearrange Eq. (7) to the form as follows:

$$\frac{\sigma}{A+B\varepsilon^n}=1-(T^*)^m \tag{8}$$

Taking the natural logarithm on both sides of Eq. (8) gives

$$\ln[1-\sigma/(A+B\varepsilon^n)]=m\ln T^* \tag{9}$$

The curves of $\ln[1-\sigma/(A+B\varepsilon^n)]$ versus $\ln T^*$ can be plotted for different strains and temperatures at reference strain rate, as shown in Fig. 5. m is the mean slope of these curves with the value of 0.6780.

After all the material constants are obtained, the Johnson−Cook model can be established as follows:

$$\sigma=(68.24-12.8971\varepsilon^{1.6093n})(1+0.1750\ln \dot{\varepsilon}^*)[1-(T^*)^{0.678}] \tag{10}$$

3.3 Modified Fields−Backofen (FB) model

The traditional formula proposed by Fields and Bachofen is widely used to describe strain-hardening behavior affected by strain-hardening exponent and strain-rate sensitivity exponent. However, the flow behavior of spray-formed 7055 aluminum alloy exhibited apparent softening phenomenon, as shown in true

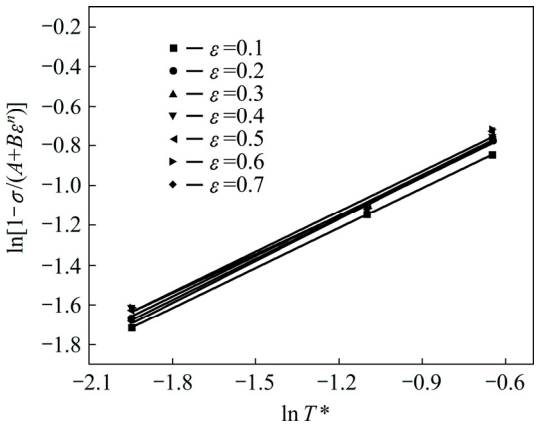

Fig. 5 Relationship between $\ln[1-\sigma/(A+B\varepsilon^n)]$ and $\ln T^*$

strain−true stress curves. Therefore, some modification must be done based on the original formula. The modified equation can be given by [14]

$$\sigma=K\cdot\varepsilon^n\cdot\dot{\varepsilon}^m\cdot\exp(bT+s\varepsilon) \tag{11}$$

where σ is the flow stress, b is a constant, K is the strength coefficient, ε is the strain, n is the strain-hardening exponent, $\dot{\varepsilon}$ is the strain rate, m is the strain rate sensitivity exponent, T is the temperature and s is the exponent for softening effect. The softening exponent s which is considered as a sum of the softening ratio can be expressed as $s=\mathrm{d}\ln\sigma/\mathrm{d}\varepsilon$. Taking the natural logarithm of both sides of Eq. (11) gives

$$\ln\sigma=\ln K+n\ln\varepsilon+m\ln\dot{\varepsilon}+bT+s\varepsilon \tag{12}$$

3.3.1 Determination of n-value

At a certain temperature, when the value of strain varies at very small amplitude, the value of $\ln K+m\ln\dot{\varepsilon}+bT+s\varepsilon$ can be simplified as a constant K_1 to make calculation of Eq. (12) easier. The formula can be rearranged as

$$\ln\sigma=n\ln\varepsilon+K_1 \tag{13}$$

Figure 6 shows the relationship of true stress versus true strain on a log−log scale. It can be seen that the curves in the uniform deformation stage are almost parallel to each other, where the slope is equal to the value of strain-hardening exponent (n). The slopes corresponding to different temperatures and strain rates can be obtained. Previous research [21] has revealed that relationships exist among value of n, the reciprocal of temperature, and strain rate on a semi-log scale under different conditions. The relationship can be assumed as

$$n=A+B\lg\dot{\varepsilon}+C/T \tag{14}$$

The mean values of parameters A, B and C can be calculated from Fig. 7. Then, the strain-hardening exponent, n, can be expressed as

$$n=0.05363\lg(\dot{\varepsilon}/\varepsilon_0)-136.18/T+0.83 \tag{15}$$

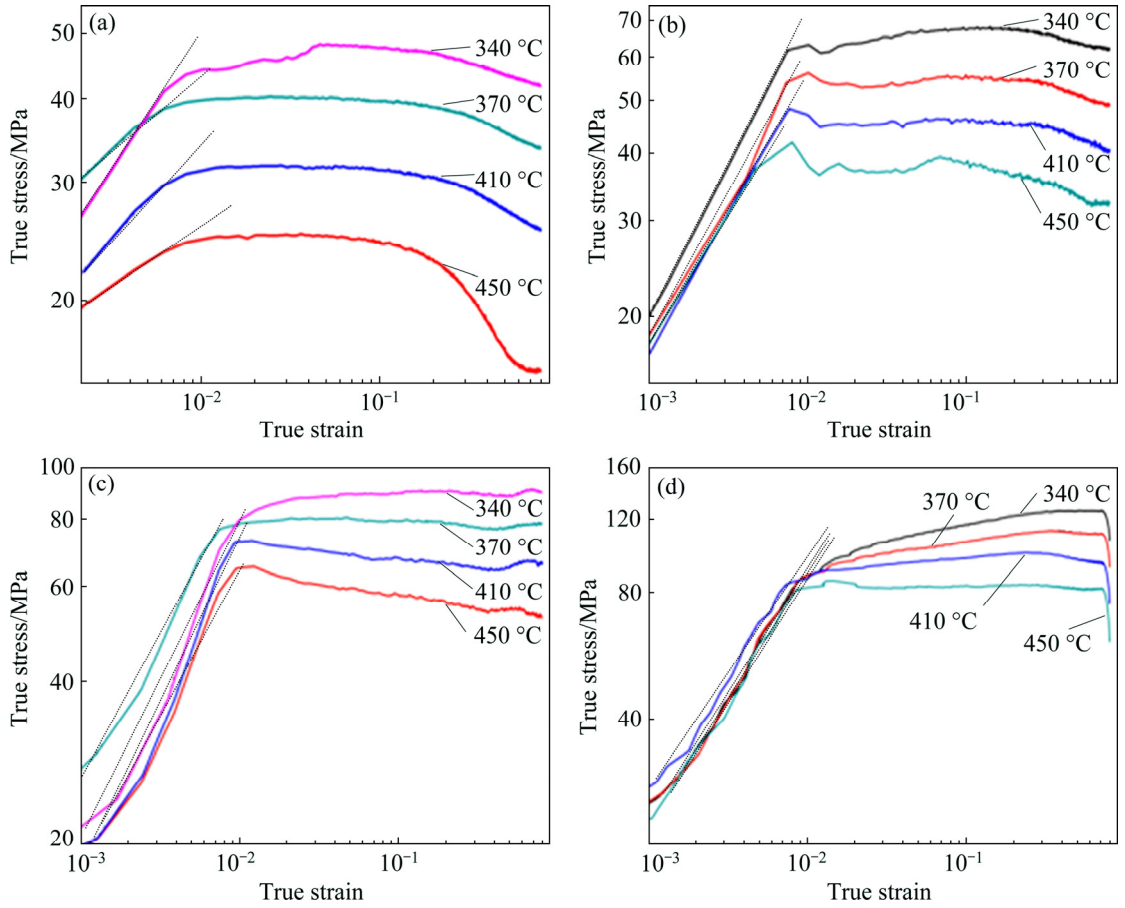

Fig. 6 Relationship between true stress and true strain of 7075 aluminum alloy at different strain rates: (a) 0.001 s^{-1}; (b) 0.01 s^{-1}; (c) 0.1 s^{-1}; (d) 1 s^{-1}

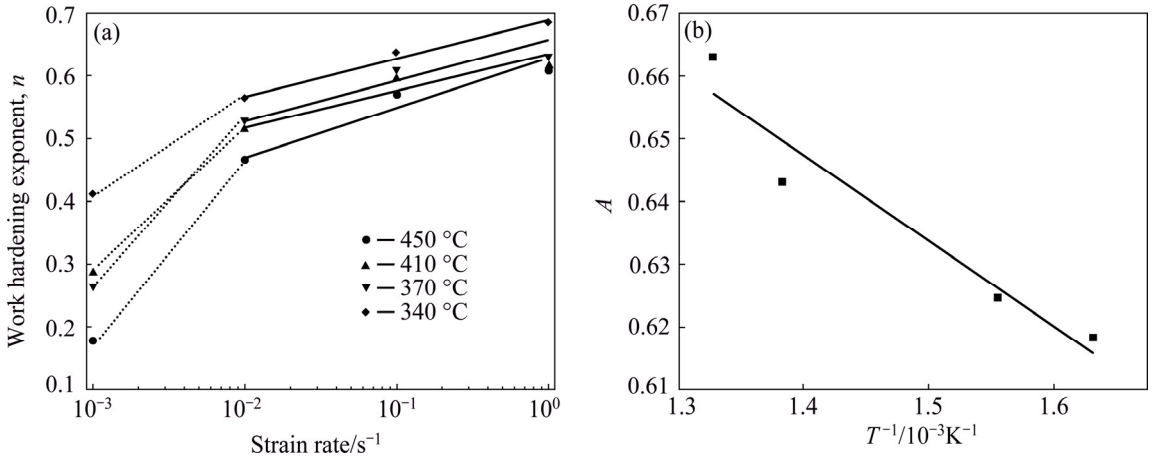

Fig. 7 Relationship between n and strain rate (a), and between parameter A and reciprocal of T (b)

3.3.2 Determination of m-value

Similar to the simplification of n-value, assuming the value of $\ln K+n\ln\varepsilon+bT+s\varepsilon$ at a certain temperature and strain rate is a constant K_2, then the following formula can be obtained from Eq. (12) as

$$\ln\sigma=m\ln\dot{\varepsilon}+K_2 \tag{16}$$

The linear relationship is found also between the strain rate sensitivity, m, and the reciprocal of temperature, as shown in Fig. 8. The value of m can be approximately obtained as

$$m=-168.76/T+0.4127 \tag{17}$$

3.3.3 Determination of b-value

It is assumed that the value of $\ln K+n\ln\varepsilon+m\ln\dot{\varepsilon}+s\varepsilon$ is a constant of K_3 at certain strain and strain rate. Then, the following formula can be given from Eq. (12):

$$\ln\sigma=bT+\ln K_3 \tag{18}$$

As shown in Fig. 9, the plots of ln σ versus T can be obtained at different strain rates, and the mean value of b is accepted to be −0.0045.

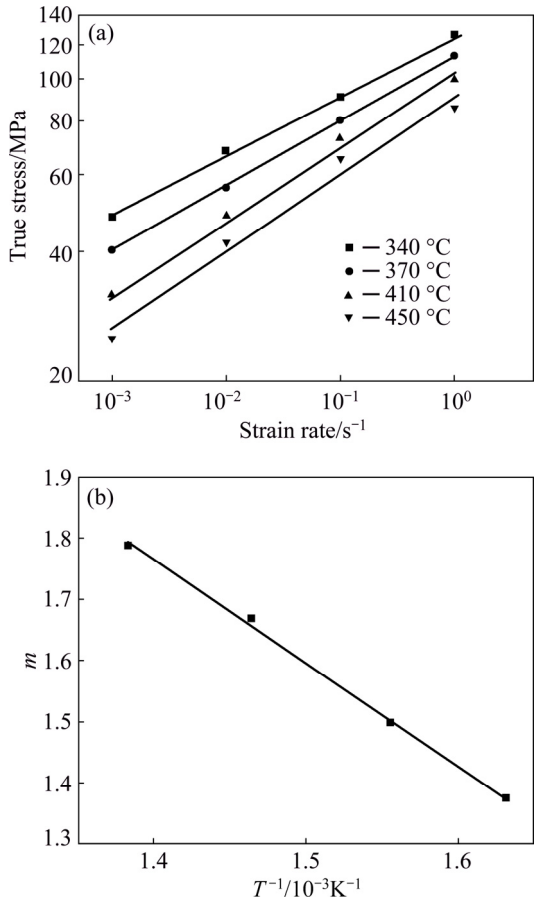

Fig. 8 Relationships between true stress and strain rate (a) and between m and reciprocal of T (b)

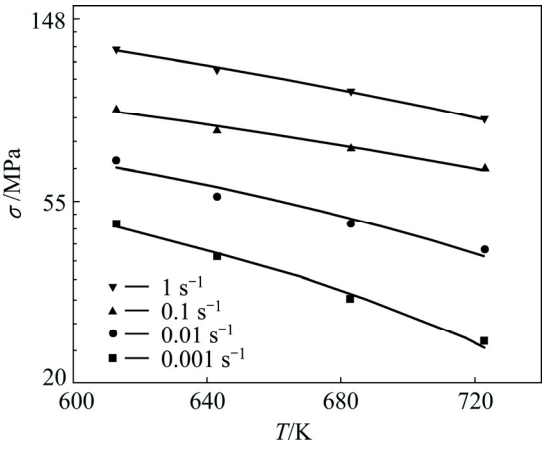

Fig. 9 Relationship between σ and T

3.3.4 Determination of s-value

In order to simplify the following calculation for the s-value, assume that the value of $\ln K+m\ln\dot{\varepsilon}+bT$ at a certain temperature and strain is a constant K_4. Then, Eq. (12) is derived as

$$\ln\sigma=n\ln\varepsilon+s\varepsilon \tag{19}$$

When the values of strain are at e^{-1} and e^{-2}, respectively, Eq. (19) can be transformed into the following equations as

$$\ln\sigma_{e^{-1}}=-n+se^{-1}+K_4 \tag{20}$$

$$\ln\sigma_{e^{-2}}=-n+se^{-2}+K_4 \tag{21}$$

Thus, the following formula can be obtained from Eqs. (20) and (21):

$$s=\frac{\ln(e^{-1}/e^{-2})-n}{e^{-1}-e^{-2}} \tag{22}$$

According to Eq. (22), the softening exponent, s, at different temperatures and strain rates can be determined. The mean value of s is accepted to be −2.374.

3.3.5 Determination of K-value

The value of K can be obtained when other parameters and experimental data were input into Eq. (11). The mean value of K is accepted to be 8359.

Then, the following formula can be obtained:

$$\sigma=8359\varepsilon^{0.83-136.18/T+0.05363\lg(\dot{\varepsilon}/\varepsilon_0)}\cdot\dot{\varepsilon}^{-168.76/T+0.4127}\cdot\exp(-0.00415T-2.374\varepsilon)$$

3.4 Arrhenius-type model

During hot compression, the constitutive equation of Arrhenius-type is one of the most widely used models to show essential relations of flow stress, strain rate and deformation temperature. Furthermore, it is also helpful to predict the flow stress at a certain condition during hot deformation. The model could be expressed as [22]

$$Z=\dot{\varepsilon}\exp[Q/(RT)] \tag{23}$$

$$\dot{\varepsilon}=AF(\sigma)\exp[-Q/(RT)] \tag{24}$$

where $\dot{\varepsilon}$ is the strain rate, Q is the activation energy, R is the mole gas constant and T is the thermodynamic temperature. And $F(\sigma)$ can be represented in three distinct forms:

$$F(\sigma)=\begin{cases}\sigma^M, & \alpha\sigma<0.8\\ \exp(\beta\sigma), & \alpha\sigma>1.2\\ [\sinh(\alpha\sigma)]^N, & \text{for all }\sigma\end{cases} \tag{25}$$

For all stress levels, the strain rate in Eq. (24) can be transformed as

$$\dot{\varepsilon}=A[\sinh(\alpha\sigma)]^N\exp[-Q/(RT)] \tag{26}$$

As shown in Figs. 10(a) and (b), a linear relationship exists between $\ln\dot{\varepsilon}$ and $\ln\sigma$ with slope of M and between $\ln\dot{\varepsilon}$ and σ with slope of β.

During deformation process, the combined effects of temperature and strain rate on deformation behavior can be expressed by Zener−Hollomon parameter as

$$Z=\dot{\varepsilon}\exp[Q/(RT)]=A[\sinh(\alpha\sigma)]^N \quad (27)$$

By taking the natural logarithm on both sides of Eq. (27), it can be expressed as

$$\ln Z=\ln\dot{\varepsilon}+Q/(RT)=\ln A+N\ln[\sinh(\alpha\sigma)] \quad (28)$$

$$Q=R\left[\frac{\partial\ln\dot{\varepsilon}}{\partial\ln[\sinh(\alpha\sigma)]}\right]_T\left[\frac{\partial\ln[\sinh(\alpha\sigma)]}{\partial(1/T)}\right]_{\dot{\varepsilon}}=RNS \quad (29)$$

The strain sensitivity N is obtained from $\partial\ln\dot{\varepsilon}$ versus $\partial\ln[\sinh(\alpha\sigma)]$ plots at different temperatures and temperature sensitivity S can be determined from $\partial\ln[\sinh(\alpha\sigma)]$ versus $\partial(1/T)$ plots at different strain rates, as demonstrated in Figs. 10(c) and (d), respectively.

Then, the value of $\ln A$ can be measured by the intercept of plots of $\ln Z$ versus $\ln[\sinh(\alpha\sigma)]$ and the value of Z can be calculated simultaneously, as shown in Fig. 11. The activation energy Q, which is an important mechanical property in the thermal deformation behavior, implies the difficulty degree of the hot deformation process [23−25]. It may provide a guideline for optimizing the hot deformation and also additional information about corresponding microstructure changes and evolution of flow stress [26]. A higher Q has usually been treated as a symbol of more difficult deforming. In addition, the softening mechanisms can also be inferred through the analysis of the activation energy. Usually, the diffusion or DRV softening mechanism dominates in the hot deformation, when the activation energy value is comparable to the self-diffusion activation energy. The Q value of this alloy is obtained to be 96.62 kJ/mol, which is lower than that of a homogenized Al−7.68Zn−2.12Mg−1.98Cu−0.12Zr, 125.4 kJ/mol [27] and that of a traditional homogenized Al−6.2Zn−0.70Mg−0.3Mn−0.17Zr, 178.85 kJ/mol [28], indicating a relatively easy hot deforming process for this alloy. Apparently, the Q value is in the range between the grain boundary diffusion energy (Q_{GB}, 82 kJ/mol) and lattice diffusion energy (Q_L, 142 kJ/mol), which means that both lattice diffusion and grain boundary diffusion exist during this process. It may be induced that the softening mechanisms are DRV and DRX.

Therefore, on basis of calculation results, the constitutive equation which describes the relationship between flow stress and strain rate at certain deformation temperature can be established as

$$\dot{\varepsilon}=6.94\times10^6[\sinh(0.01508\sigma)]^{4.804}\exp\left(-\frac{96620}{8.314T}\right)$$

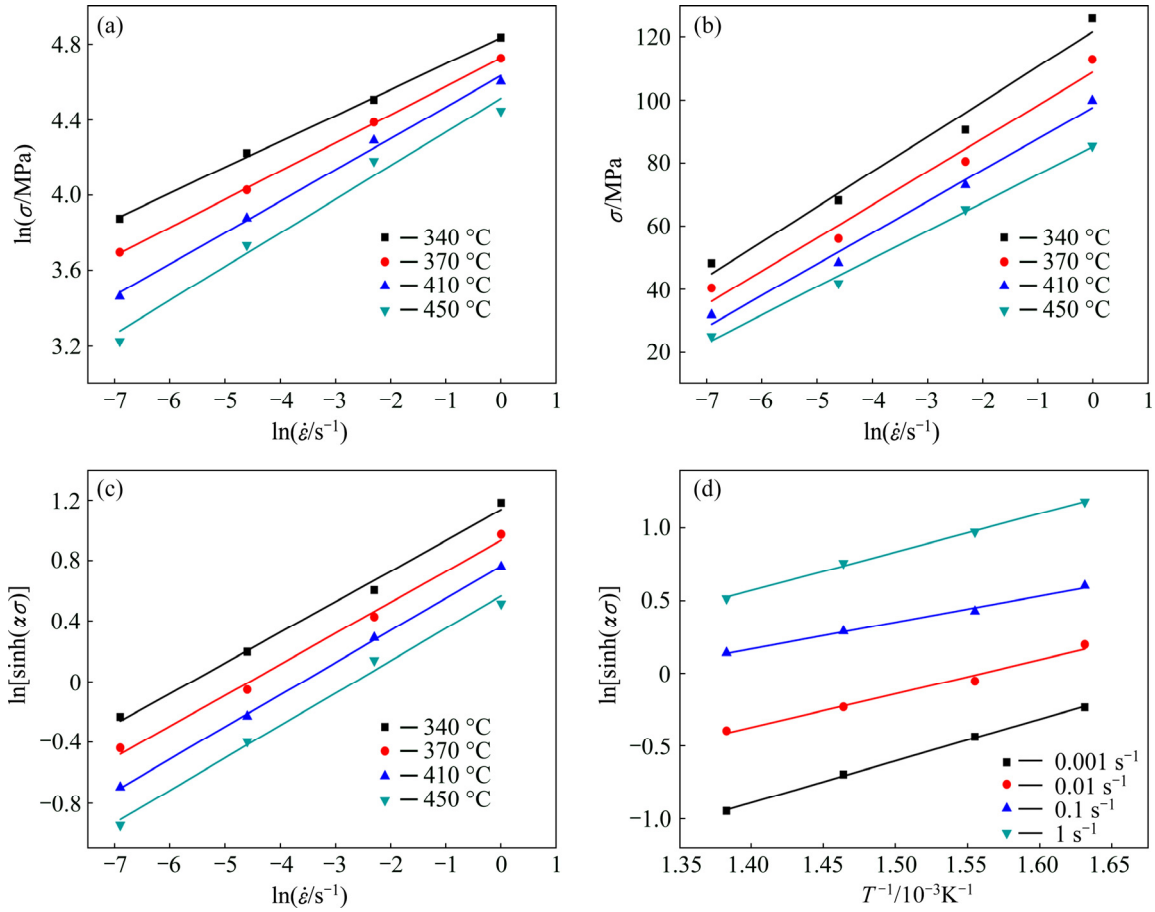

Fig. 10 Linear fittings of flow properties of 7075 aluminum alloy: (a) $\ln\sigma-\ln\dot{\varepsilon}$; (b) $\sigma-\ln\dot{\varepsilon}$; (c) $\ln[\sinh(\alpha\sigma)]-\ln\dot{\varepsilon}$; (d) $\ln[\sinh(\alpha\sigma)]-T^{-1}$

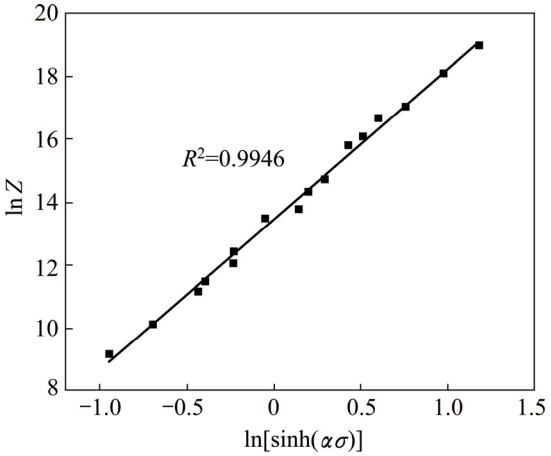

Fig. 11 Linear relationship between ln Z and ln[sinh($\alpha\sigma$)]

3.5 Analysis of constitutive equation accuracy

The comparisons between predicted flow stresses and experimental flow stresses at different temperatures of these three models are shown in Fig. 12. In general, the deviation of Arrhenius-type is the smallest for introducing Z parameter to combine the influence of strain rate and temperature. Therefore, it has relatively high accuracy in the wide deformation temperature and strain rate ranges. It can also be seen from Fig. 12 that the predicted and experimental values of JC model exhibit large deviation, except under or close to the referenced deformation conditions. With the gradual variation in strain rate or deformation temperature, the amplitude broadens. This is because this model assumes that the effect of strain rate and temperature on deformation is isolated. Such relationship becomes more obvious as the temperature or strain rate changes. This model is not applicable at high temperature or high strain rate for this alloy (Fig. 12(d)). It can be easily seen that FB model gets the best accuracy at temperature of 340 °C, as shown in Fig. 12(a). However, the deviation becomes larger with the increase of the temperature. The model can be well used to describe the strain hardening behavior. Deformed at low temperature, the softening processes of this alloy are inhabited. Therefore, the accuracy at low temperature is good. The deviation at high temperature can be attributed to the occurrence of DRX.

The predictive power of these three phenomenological constitutive models can be presented by relative errors, correlation coefficient (R) and average absolute relative error (AARE). Figure 13 displays the correlations between the experimental flow stresses and predicted ones by the three models over the complete

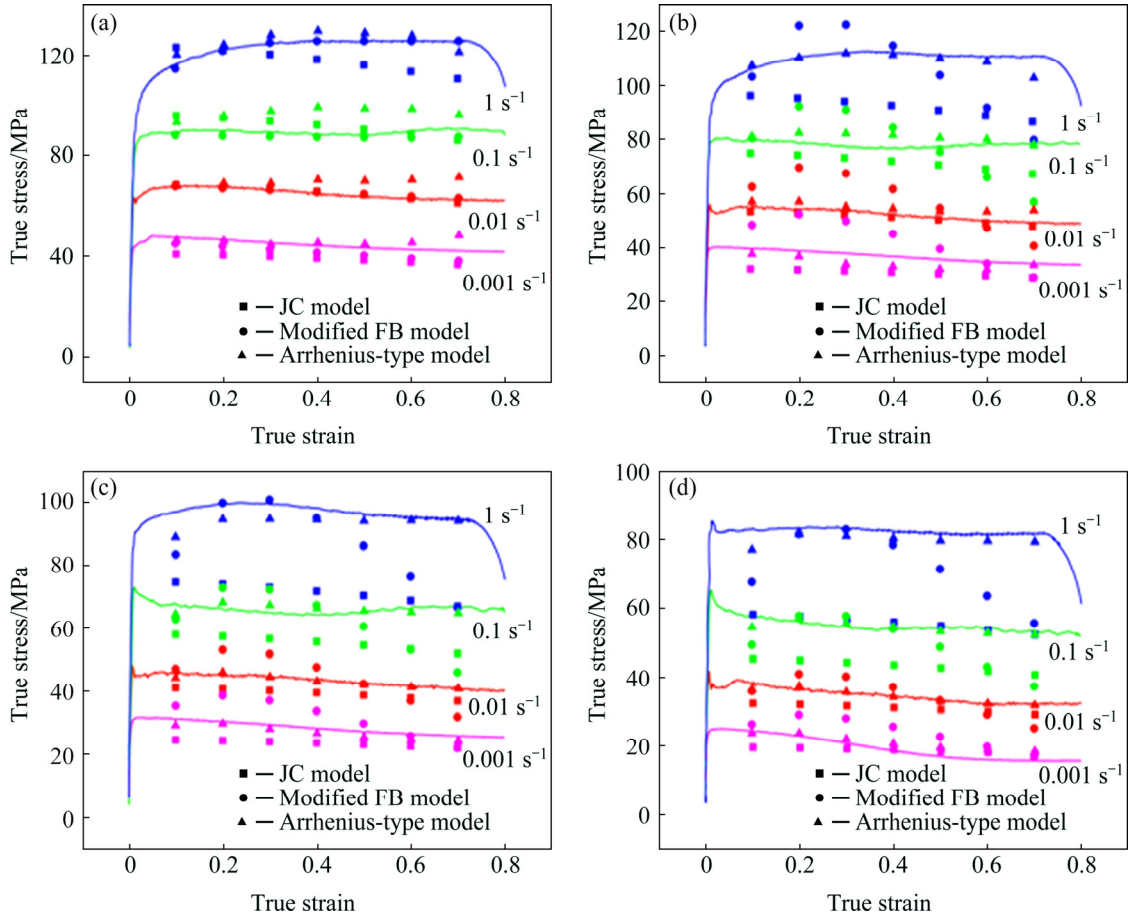

Fig. 12 Relationship between predicted flow stress and experimental flow stress at different temperatures: (a) 340 °C; (b) 370 °C; (c) 410 °C; (d) 450 °C

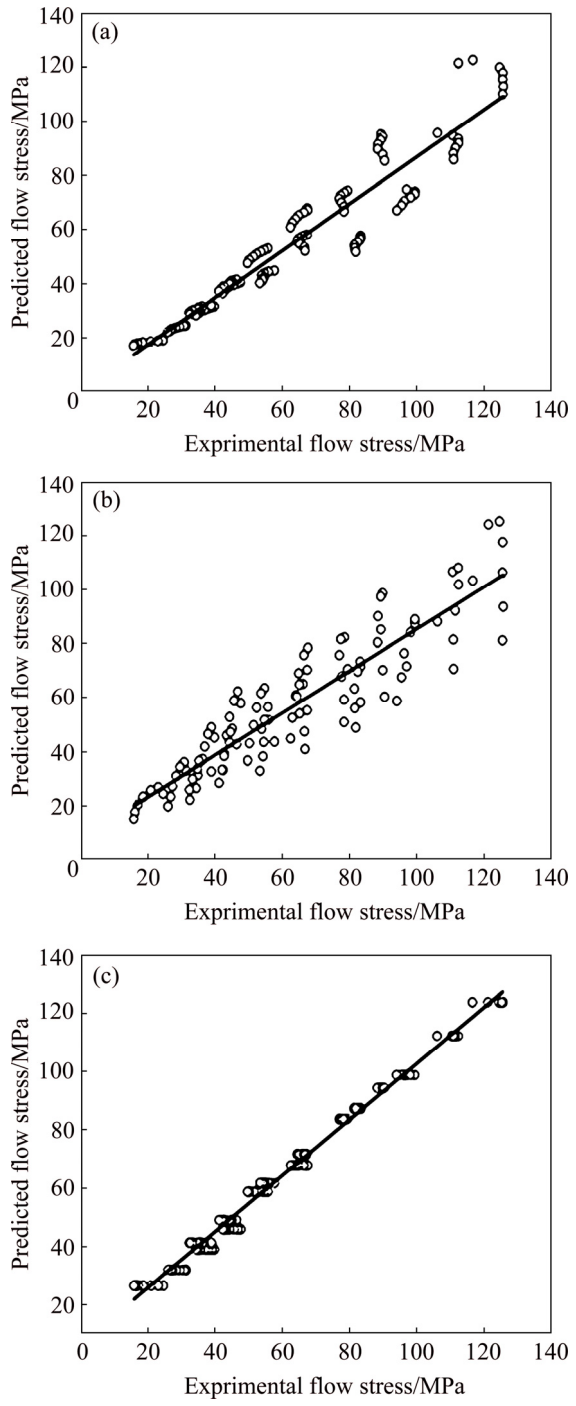

Fig. 13 Correlations between experimental flow stresses and predicted ones: (a) JC model; (b) Modified FB model; (c) Arrhenius-type model

range of processing variables. Obviously, most of the data points predicted by Arrhenius-type are close to the line with slope fixed to be 1 (Fig. 13(c)), whereas the deviation of the modified FB model is the largest (Fig. 13(b)). The R values of JC model, modified FB model and Arrhenius-type are 0.910, 0.832 and 0.991, respectively. These mean that the Arrhenius-type has better correlation than other two models.

The AARE values at different strains are shown in Fig. 14(a). The AAREs calculated from the Arrhenius-type model are obviously lower compared with others in nearly all the strain range. And modified FB model exhibits a sharp increase, indicating poor prediction ability at large strain. What is more, JC model shows a plat variation with the AARE values between 0.12 and 0.15. This means that a large deviation keeps in the strain range. Furthermore, as shown in Fig. 14(b), the relative errors of JC model, modified FB model and Arrhenius-type model are in the ranges from −0.367 to 0.0914, from −0.404 to 0.331 and from −0.0354 to 0.689, respectively. The JC model has a narrower gap compared with others. However, Fig. 14(b) shows that Arrhenius-type model is more concentrated and modified FB model is the widest.

As discussed above, Arrhenius-type model exhibits the best performance to predict the hot deformation behavior of spray-formed 7055 aluminum alloy among these three models.

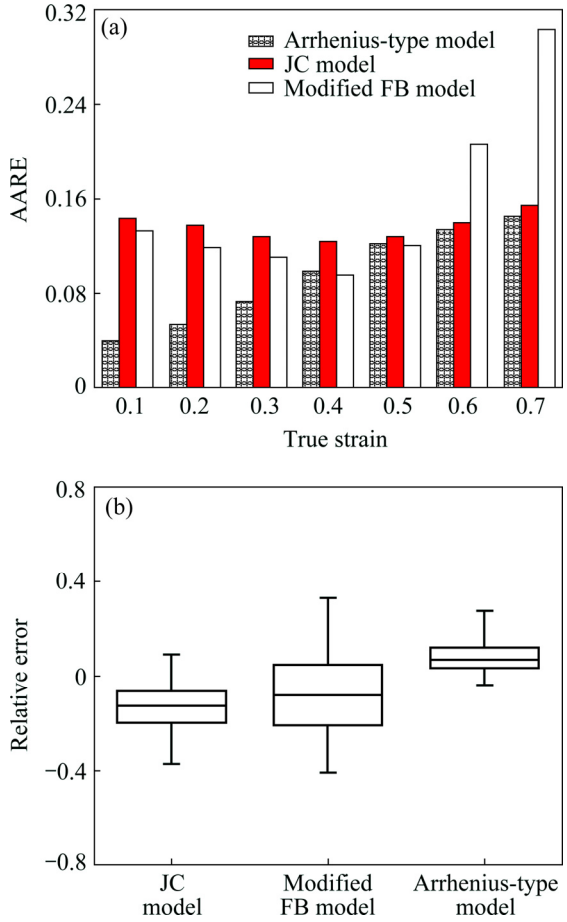

Fig. 14 Comparisons of three models: (a) AARE; (b) Statistical analysis

4 Conclusions

1) The flow stress decreases with increasing temperature and decreasing strain rate.

2) Three phenomenological models of JC model, modified FB model and Arrhenius-type model were used to describe the hot deformation behavior of the spray-formed 7055 alloy. Among these models, JC and modified FB models could not well predict the flow stress due to the isolated calculation in temperature and strain rate.

3) It has been validated through relative errors, correlation coefficient (R), average absolute relative error (AARE) and statistical analysis that Arrhenius-type has the best prediction accuracy.

4) Through the analysis in Q value of Arrhenius-type model, it can be suggested that this alloy has a relatively easy deformation and the softening mechanisms include DRV and DRX.

References

[1] BIST A, SAINI J S, SHARMA B. A review of tool wear prediction during friction stir welding of aluminium matrix composite [J]. Transactions of Nonferrous Metals Society of China, 2016, 26(8): 2003−2018.

[2] RAO A C U, VASU V, GOVINDARAJU M, SRINADH K V S. Stress corrosion cracking behaviour of 7xxx aluminum alloys: A literature review [J]. Transactions of Nonferrous Metals Society of China, 2016, 26(6): 1447−1471.

[3] ROMETSCH P A, ZHANG Y, KNIGHT S. Heat treatment of 7xxx series aluminium alloys—Some recent developments [J]. Transactions of Nonferrous Metals Society of China, 2014, 24(7): 2003−2017.

[4] LIN Yong-cheng, CHEN Xiao-min. A critical review of experimental results and constitutive descriptions for metals and alloys in hot working [J]. Materials & Design, 2011, 32: 1733−1759.

[5] GAMBIRASIO L, RIZZI E. On the calibration strategies of the Johnson−Cook strength model: Discussion and applications to experimental data [J]. Materials Science and Engineering A, 2014, 610(7): 370−413.

[6] BUZYURKIN A E, GLADKY I L, KRAUS E I. Determination and verification of Johnson−Cook model parameters at high-speed deformation of titanium alloys [J]. Aerospace Science and Technology, 2015, 45(1): 21−27.

[7] ZHANG Ding-ni, SHANGGUAN Qian-qian, XIE Can-jun, LIU Fu. A modified Johnson−Cook model of dynamic tensile behaviors for 7075-T6 aluminum alloy [J]. Journal of Alloys and Compounds, 2015, 619(15): 186−194.

[8] AKBARI Z, MIRAZADEH H, CABRERA J M. A simple constitutive model for predicting flow stress of medium carbon microalloyed steel during hot deformation [J]. Materials & Design, 2015, 77: 126−131.

[9] JOHNSON G R, COOK W H. A constitutive model and data for metals subjected to large strains, high strain rates and high temperatures [C]//Proceedings of the 7th Symposium Ballistics. Den Haag. The Netherland, 1983: 541−547.

[10] JIA Wei-tao, XU Shuang, LE Qi-chi, FU Li, MA Li-feng, TANG Yan. Modified Fields−Backofen model for constitutive behavior of as-cast AZ31B magnesium alloy during hot deformation [J]. Materials & Design, 2016, 106: 20−32.

[11] CHEN Wei, GUAN Ying-ping, WANG Zhen-hua. Modeling of flow stress of high titanium content 6061 aluminum alloy under hot compression [J]. Journal of Materials Engineering and Performance, 2016, 25(9): 4081−4088.

[12] DONG Yuan-yuan, ZHANG Cun-sheng, LU Xing, WANG Cui-xue, ZHAO Guo-qun. Constitutive equations and flow behavior of an as-extruded AZ31 magnesium alloy under large strain condition [J]. Journal of Materials Engineering and Performance, 2016, 25(6): 2267−2281.

[13] BAKTASH R, MIRZADEH H. A simple constitutive model for prediction of single-peak flow curves under hot working conditions [J]. Journal of Engineering Materials and Technology, 2016, 138(2): 021004-1−021004-5.

[14] TAKUDA H, MORISHITA T, KINOSHITA T, SHIRAKAWA N. Modelling of formula for flow stress of a magnesium alloy AZ31 sheet at elevated temperatures [J]. Journal of Materials Processing Technology, 2005, 164(12): 58−62.

[15] QUAN Guo-zheng, LIU Ke-wei, ZHOU Jie, CHEN Bin. Dynamic softening behaviors of 7075 aluminum alloy [J]. Transactions of Nonferrous Metals Society of China, 2009, 19(5): 37−41.

[16] QIN Fang-cheng, LI Yong-tang, JU Li. A comparative study of hot deformation behaviors for sand casting and centrifugal casting Q235B flange blanks [J]. High Temperature Materials and Processes, 2017, 36(3): 209−221.

[17] SHALBAFI M, ROUMINA R, MAHMUDI R. Hot deformation of the extruded Mg−10Li−1Zn alloy: Constitutive analysis and processing maps [J]. Journal of Alloys and Compounds, 2017, 696(12): 69−77.

[18] TRIMBLE D, SHIPLEY H, LEA L, JARDINE A, O'DONNELL G E. Constitutive analysis of biomedical grade Co−27Cr−5Mo alloy at high strain rates [J]. Materials Science and Engineering A, 2017, 682(4): 66−74.

[19] YAN Jie, PAN Qing-lin, LI Bo, HUANG Zhi-qi, LIU Zhi-ming, YIN Zhi-min. Research on the hot deformation behavior of Al−6.2Zn−0.70Mg−0.3Mn−0.17Zr alloy using processing map [J]. Journal of Alloys and Compounds, 2015, 632(5): 49−57.

[20] VURAL M, CARO J. Experimental analysis and constitutive modeling for the newly developed 2139-T8 alloy [J]. Materials Science and Engineering A, 2009, 520(1−2): 56−65.

[21] TSAO L C, CHEN C H, WU R W, CHANG S Y, CHEN R S. Plastic flow behavior, microstructure, and corrosion behavior of AZ61 Mg alloy during hot compression deformation [J]. Journal of Manufacturing Processes, 2015, 18(1): 67−74.

[22] LI Bo, PAN Qing-lin, YIN Zhi-min. Characterization of hot deformation behavior of as-homogenized Al−Cu−Li−Sc−Zr alloy using processing maps [J]. Materials Science and Engineering A, 2014, 614(4): 199−206.

[23] MIRZADEH H, CABRERA J M, NAJAFIZADEH A. Constitutive relationships for hot deformation of austenite [J]. Acta Materialia, 2011, 59(16): 6441−6448.

[24] MIRZADEH H. Simple physically-based constitutive equations for hot deformation of 2024 and 7075 aluminum alloys [J]. Transactions of Nonferrous Metals Society of China, 2015, 25(5): 1614−1618.

[25] MIRZADEH H, ROOSTAEI M, PARSA M H, MAHMUDI R. Rate controlling mechanisms during hot deformation of Mg−3Gd−1Zn magnesium alloy: Dislocation glide and climb, dynamic recrystallization, and mechanical twinning [J]. Materials & Design, 2015, 68: 228−231.

[26] MIRZADEH H. Quantification of the strengthening effect of reinforcements during hot deformation of aluminum-based composites [J]. Materials & Design, 2015, 65: 80−82.

[27] FENG DI, ZHANG Xin-ming, LIU Sheng-dan, DENG Yun-lai. Constitutive equation and hot deformation behavior of homogenized Al−7.68Zn−2.12Mg−1.98Cu−0.12Zr alloy during compression at elevated temperature [J]. Materials Science and Engineering A, 2014, 608(25): 63−72.

[28] YAN Liang-ming, Shen Jian, LI Jun-peng, LI Zhou-bing, YAN Xiao-dong. Deformation behavior and microstructure of an Al−Zn−Mg−Cu−Zr alloy during hot deformation [J]. International Journal of Minerals, Metallurgy, and Materials, 2010, 17(1): 46−52.

通过唯相学模型预测喷射成形 7055 铝合金的热变形行为

王向东[1]，潘清林[1]，熊尚武[2]，刘丽丽[1]，孙元伟[1]，王维裔[1]

1. 中南大学 材料科学与工程学院，长沙 410083；
2. 中南大学 轻合金研究院，长沙 410083

摘　要：通过高温热压缩实验研究喷射成形 7055 铝合金的热变形行为，实验温度为 340~450 °C，应变速率为 0.001~1 s^{-1}。将 Johnson−Cook 模型、改良 Fields−Backofen 模型和 Arrhenius 模型应用在该合金的热变形行为研究中，对这 3 种模型进行相对误差、相关系数以及平均相对误差的绝对值的比较研究。结果表明，Johnson−Cook 模型和改良 Fields−Backofen 模型由于在线性拟合过程中产生较大偏差，不能精确预测该合金的热变形行为；Arrhenius 模型则因为将温度和应变速率的作用有效结合，得到较好的预测效果。

关键词：喷射成形 7055 铝合金；热变形行为；唯相学模型；统计分析

(Edited by Bing YANG)